

https://dspace.org/

Rotational barriers in Nmethylcinnamoylchloroquine analogues Variable temperature NMR spectroscopy and DFT studies

Mpelegeng V. Bvumbi; Memory Zimuwandeyi; Anza I. Nemudzivhadi; Mwadham M. Kabanda

https://hdl.handle.net/10539/46236
WOS

Downloaded from a DSpace repository. https://dspace.org/

Journal of Molecular Structure 1335 (2025) 141943

Contents lists available at ScienceDirect

Journal of Molecular Structure

journal homepage: www.elsevier.com/locate/molstr

Rotational barriers in *N*-methyl-cinnamoyl-chloroquine analogues: Variable temperature NMR spectroscopy and DFT studies

Mpelegeng V. Bvumbi [a,*], Memory Zimuwandeyi [b], Anza I. Nemudzivhadi [a], Mwadham M. Kabanda [a]

[a] Department of Chemistry, Faculty of Science, Engineering and Agriculture, University of Venda, Private Bag X 5050, Thohoyandou 0950, Republic of South Africa
[b] Molecular Sciences Institute, School of Chemistry, University of the Witwatersrand, Private Bag X 3, Wits 2050, Republic of South Africa

ARTICLE INFO

Keywords:
N-methyl-cinnamoyl chloroquinoline
Rotamers
VT NMR
Barrier height
Relative stability

ABSTRACT

The study of the rotational barrier of the amide bond (C(=O)– N) by nuclear magnetic resonance (NMR) and theoretical evaluation using the density functional theory (DFT) was investigated. Three new *(E)*-(3-((7-chloroquinolin-4-yl)amino)propyl)-*N*-methylacrylamides with variation of substitution on the aromatic ring were investigated. The dynamic NMR study shows restricted rotation around the amide bond resulting in the structures exhibiting a pair of rotamers (*syn*– and *anti*–). The reaction mechanism showing the formation of the tertiary acrylamide at room temperature from the reactant species was performed, using DFT/ M06–2X/ 6-311++G(d,p) method. Furthermore, the *anti*– and the *syn*– rotamers about the amide bond were investigated for each compound, using the same DFT method, to identify the relative stability of rotamers as well as the barrier height for their interconversion. The investigation was performed in different media, including vacuum, methanol, and aqueous media. The results suggest that the rotamers for each investigated molecule have minimal energy difference so that both the *anti*– and the *syn*– rotamers can be considered to co-exist in different media. An independent investigation of the secondary acrylamide suggests that the relative stability of the *anti*– and the *syn*– conformational rotamers favour only the formation of the *anti*–rotamer.

1. Introduction

The continuous emergence of multidrug-resistant microorganisms is a serious threat to public health. As a result, any model of drug design that promises to address the rising problem of drug resistance is needed [1]. The hybrid drug concept, especially in malaria, has been researched in the hope of fighting multidrug-resistant *P. falciparum* infections. Extensive reviews have been published relating to the synthesis and biological activities of antimalarial hybrid molecules addressing drug resistance, potency, toxicity, pharmacokinetics, metabolism, solubility, and mode of administration [2–4]. One of the reported antimalarial hybrids is the quinoline-cinnamic acids, Fig. 1. Authors discovered that the linker to the quinoline and cinnamic acid fragments was crucial for the activity [5,6].

In particular, the replacement of the dipeptide linker by amino-amide significantly improved the antiplasmodial activities [5]. In our lab, we have been synthesizing quinoline-cinnamic hybrids using different amino-amide linkers (straight and branched) and different functional groups on the cinnamic ring and studying their structural, physical, and antiplasmodial properties (unpublished data).

The resulting functional group of quinoline-cinnamic hybrid with amino-amide linkers is acrylamide. Acrylamides on their own are known to be important building blocks in chemistry and medicine. Generally, they have effects in several applications such as siliceous composite structures, in biology for electrophoresis, removal of dissolved metallic nanoparticles from water, gene delivery devices, etc. [7,8]. The different behavioural patterns of *N*-methyl acrylamide which resulted in a pair of rotamers interested us hence their investigations in this study.

Rotamers are different conformations of a molecule that result from the rotation around a single bond. Ordinarily, and in Nuclear Magnetic Resonance (NMR), the rotamers cannot be isolated because of fast interconversion at room temperature meaning only the average of the rapidly equilibrating conformers is observable [9–12]. However, when there is a high rotational energy barrier between conformers, as is the case for the *anti*– and *syn*– conformers, it is possible to observe their presence in the solution during the same NMR measurements. For

* Corresponding author.
E-mail address: mpelegeng.bvumbi@univen.ac.za (M.V. Bvumbi).

https://doi.org/10.1016/j.molstruc.2025.141943
Received 12 November 2024; Received in revised form 14 February 2025; Accepted 3 March 2025
Available online 4 March 2025
0022-2860/© 2025 The Author(s). Published by Elsevier B.V. This is an open access article under the CC BY-NC-ND license (http://creativecommons.org/licenses/by-nc-nd/4.0/).

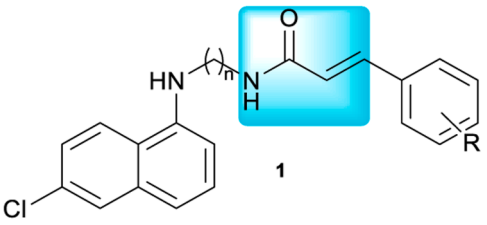

Fig. 1. Skeleton structure of conjugated cinnamoylated-chloroquinoline (CQ) compound.

instance, the combination of density functional theory (DFT) modeling and low-temperature NOE assignment of rotamers about the C–N amide bond showed the existence of non-covalent interaction between the *N*-acyl piperidine and the amide carbonyl, resulting in distinct conformers being observed, Fig. 2a [13].

The use of NMR spectroscopy to study restricted rotation in amides has been anciently explored [14–18]. The experimental methods on NMR include variable NMR [19,20], exchange spectroscopy NMR [21, 22], and NMR line shape analysis [23,24].

The rotational barriers determined by dynamic NMR spectroscopy indicate that the chemical nitrogen protons exchange as the C–N amide bond rotates. Furthermore, the effect of hindrances to the free rotation brought by different groups can stipulate the mixtures of conformers at ordinary temperatures, Fig. 2b [25].

It is noted that functionally substituted amides that bring the rotational *anti*– and *syn*– isomerism have been studied for a long time [26–29]. However, the study of acrylamides is limited. Recently, Larina *et al.* studied the rotational isomerism of functionally substituted acrylamides by dynamic NMR spectroscopy and found that in solution, they are in the form of *Z* – and *E* – isomers with *E* – rotamer being the predominant form, Fig. 2c [30].

Our newly synthesized acrylamides bearing *N*-methyl group showed interesting results compared to their unsubstituted analogues hence worthy of further investigation. Not only did they exhibit the mixture of rotamers at room temperature Fig. 2d, but they also showed the conformational change arising under thermal conditions. Amide bonds have been shown to exhibit rotamers due to restricted rotation arising from the partial double bond character of the C–N amide bond [31]. The lone pair of electrons on nitrogen conjugate with the carbonyl moiety leading to planarity at the nitrogen center. This conformation leads to the formation of *anti* – and *syn*– rotamers detectable by NMR. This phenomenon is sometimes observed in C–N amide bond-containing compounds as observed in our compound library. In addition to the variable NMR, the computational approach was used to evaluate the influence of the methyl group at the *N*- substituent on the rotational barrier. Therefore, the Density Functional Theory (DFT) approach was utilized herein to obtain the rotamers, as a result of variation of the C-N-C=O torsion angle, and to compare their energetic stabilities. For interest's sake, the presentation of results for the secondary amide is also reported to identify the structural differences with the tertiary acrylamide structures.

2. Experimental

2.1. Materials

All chemicals (from Merck) and solvents (from Murula) were used without any further purification.

2.2. Instrumentation

Bruker Optics 7.0 Alpha Fourier transformed Infrared (FTIR) spectrophotometer was used to study the functional groups and the absorptions were reported using the wavenumber scale in the 500–4000 cm-1 range. ^{1}H NMR and ^{13}C NMR spectra were recorded on a Bruker 400 MHz spectrometer at 27 °C–90 °C in dimethyl sulfoxide (DMSO-d6) in the presence of tetramethylsilane (TMS) as internal standard. The melting points were determined by Electrothermal 9200 Büchi LABOTEC melting point (B-5400) using a capillary tube. The masses were determined by Tandem MS (MS/MS) experiments, typical mass accuracies with a mass error below 1 ppm were obtained using a mass calibration solution of sodium iodide (NaI). High resolution was obtained for MS and (MS/ MS) experiments using a mass-to-ratio (m/z) range of 100–1000. Argon gas was used as a collision gas for (MS/MS) experiments along with MSE mode using a collision energy ramp of 12 eV to 25 eV for the generation of fragments.

2.3. Synthesis

Synthesis of cinnamoylated chloroquinoline analogues

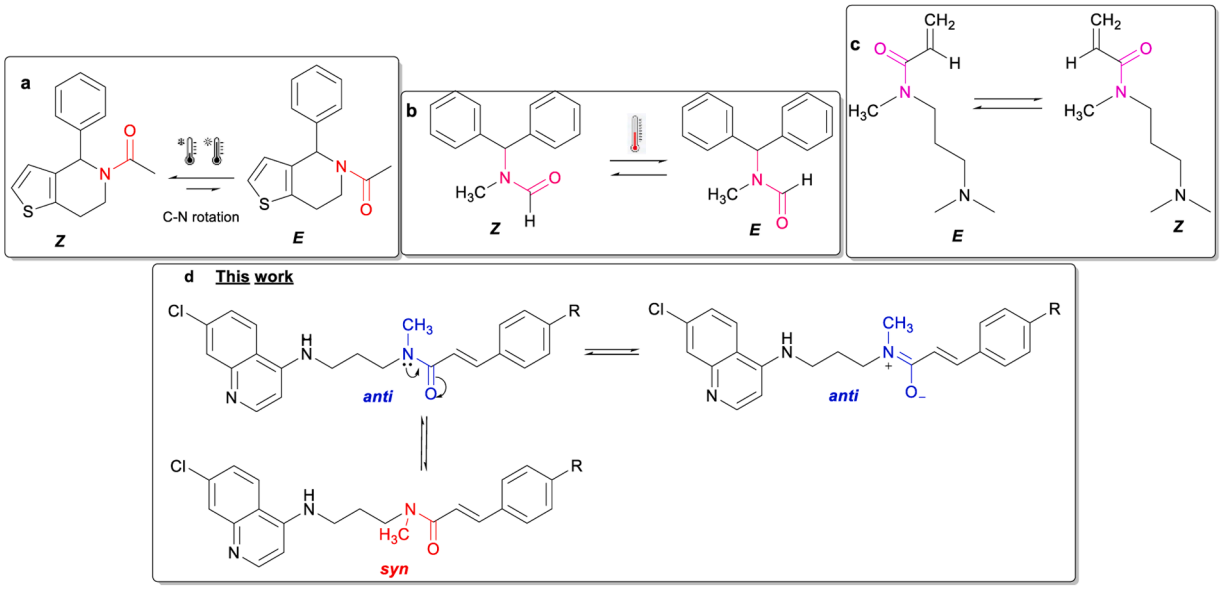

Fig. 2. Thermal-induced bond rotation. (**a**) Observed thermal C-N bond rotation [13], (**b**) C-N bond rotation due to increased temperatures [25], (**c**) C-N bond rotation of acrylamides [30], **d**) The effect of the bulky methyl group in the C-N rotation, a novel effect on these compounds.

Synthesis of intermediate **2** was achieved by the nucleophilic substitution at the 4th position of commercially available 4,7-dichloroquinoline with propyl-diamine. On the other hand, acid chloride, **4** was prepared from trans-cinnamic acids, **3** in the presence of toluene and dimethyl formamide to give cinnamoylated chloroquinoline analogues (**5-6**) [32] (which were synthesized as follows:)

A mixture of N-(7- chloroquinoline 4yl) alkyl-diamine, **2** (1.0 equiv.), triethylamine (TEA) (3.0 equiv.) and 15 mL dry DCM was stirred at room temperature for 15 min. Then, a solution of cinnamoyl chloride (**4**) and dry DCM was added dropwise. The reaction mixture was stirred at room temperature for 18 h, light-protected. The progress of the reaction was monitored by thin-layer chromatography (TLC). After completion, the solvent was evaporated from the mixture under reduced pressure. The residue was dissolved in ethyl acetate/5 % NaOH mixture (1:1). The reaction was taken up by liquid-liquid extraction using 5 % NaOH and washed with water. The organic layer was dried over anhydrous magnesium sulphate, filtered and excess solvent was removed under reduced pressure before being purified by column chromatography using 5–30 % (v/v) ethyl acetate/methanol followed by crystallization with hot ethanol to afford compounds **5-6** as light-yellow solid/crystals.

2.3.1. Synthesis of N-(3-((7-chloroquinolin-4-yl) amino)propyl) cinnamamide (5)

^{1}H NMR (400 MHz, DMSO-d$_6$) δ 8.39 (d, *J* = 5.4 Hz, 1H, H-3), 8.28-8.24 (m, 2H, H-9, NH-15), 7.79 (d, *J* = 2.2 Hz, 1H, H-6), 7.56 (d, *J* = 6.8 Hz, 2H, H-20), 7.48–7.32 (m, 6H, H-21, H-18, H-8, H-22, NH-11), 6.64 (d, *J* = 15.8 Hz, 1H, H-17), 6.49 (d, *J* = 5.5 Hz, 1H, H-2), 3.33 (dd, *J* = 12.6, 6.6 Hz, 4H, H-12; H-14), 1.87 (p, *J* = 6.8 Hz, 2H, H-13). **^{13}C NMR (101 MHz, DMSO-d$_6$)** δ 165.2 (C-16), 151.9 (C-3), 150.1 (C-4), 149.0 (C-5), 138.6 (C-18), 134.9 (C-19), 133.4 (C-7), 129.4 (C-6), 128.9 (C-20), 127.5 (C-21), 127.4 (C-22), 124.1 (C-9), 124.0 (C-8) 122.2 (C-17), 117.5 (C-10), 98.7 (C-2), 40.1 (C-14), 36.7 (C-12), 27.9 (C-13). **IR (cm^{-1})**: 3337 (N-H stretch), 3048 (C-H stretch), 1659 (C=O), 1622 (C=N), 1537.19 (C=C), 1137.7 (C-N). **HRMS(ESI-TOF+)**: *m/z* Calculated for $C_{21}H_{20}ClN_3O$:365.8560; found: 366.1408 (M+H). **mp**. 190-196 °C.

2.3.2. Synthesis of N-(3-((7-chloroquinolin-4-yl)amino)propyl)-N-methylcinnamamide (6a)

^{1}H NMR (400 MHz, DMSO) δ 8.41 (d, *J* = 5.4 Hz, 0.49H) and 8.36 (d, *J* = 5.4 Hz, 0.56H, H-3), 8.32 (d, *J* = 9.0 Hz, 0.55H) and 8.26 (d, *J* = 9.0 Hz, 0.46H, H-9), 7.79 (d, *J* = 2.2 Hz, 1H, H-6), 7.67 (d, *J* = 6.8 Hz), 7.55–7.26 (m, 6H), 7.25–7.15 (m, 2H), 7.05 (d, *J* = 15.4 Hz, 0.30H, H-18), 7.03 (s, 0.24H), 6.49 (d, *J* = 5.5 Hz, 1H, H-2), *syn- rotamer*, 3.67 (t, *J* = 7.2 Hz, 1.15H) and *anti- rotamer*, 3.53 (t, *J* = 7.0 Hz, 0.89H, H-14), 3.34–3.24 (m, 2H, H-12), *anti- rotamer,* 3.18 (s, 1.35H) and *syn- rotamer,* 2.96 (s, 1.61H, H-16), *syn- rotamer*, 2.00 (p, *J* = 6.9 Hz, 1.16H) and *anti-rotamer,* 1.91 (p, *J* = 7.2 Hz, 0.92H, H-13). **^{13}C NMR (101 MHz, DMSO)** δ 166.2 and 165.9 (C-17), 152.3 (C-3), 150.6 (C-1) 149.4 (C-5), 141.7 and 141.5 (C-19), 135.6, 135.4 (C-20), 133.9 (C-7), 129.9, 129.8, 129.2, 128.9, 128.4, 128.1, 127.9, (C21, C-22, C-23), 127.4, (C-6) 124.6 (C-9 and C-8), 124.4 (C-9), 119.1 and 118.5 (C-18), 117.9 (C-10), 99.2 and 99.1 (C-2), *syn- rotamers,* 47.2, and *anti- rotamer,* 45.8 (C-14), 40.6 and 40.2 (C-12), *anti- rotamer,* 35.7, and *syn- rotamer,* 34.1 (C-16), *syn-rotamer,* 27.6, and *anti- rotamer,* 26.2 (C-13). **IR (cm^{-1})** 3333 (N-H stretch), 3059 (aromatic C-H stretch), 1644 (C=O), 1575 (C=C), 1137 (C-N stretch quinoline), 761 (C-N stretch). **HRMS(ESI-TOF+)**: *m/z* Calculated for $C_{22}H_{22}ClN_3O$: 379.1451; found: 378.1376 (M-H). **mp**. 118–120 °C.

2.3.3. Synthesis of (E)-3-(4-chlorophenyl)-N-(3-((7-chloroquinolin-4-yl) amino)propyl)-N-methylacrylamide (6b)

^{1}H NMR (400 MHz, DMSO) δ 8.40 (d, *J* = 5.5 Hz, 0.46H) and 8.34 (d, *J* = 5.4 Hz, 0.59H, H-3), 8.30 (d, *J* = 9.0 Hz, 0.56H) and 8.25 (d, *J* = 9.0 Hz, 0.51H H-9), 7.82 – 7.71 (m, 2H), 7.52–7.37 (m, 4H) and 7.37–7.26 (m, 2H), 7.25–7.17 (m, 1.52H), 7.05 (d, *J* = 15.4 Hz, 0.54H, H-18), 6.48 (d, *J* = 5.4 Hz, 0.40H) and 6.45 (d, *J* = 5.4 Hz, 0.60H, H-2), 3.66 (t, *J* = 7.1 Hz, 1.10H) and 3.52 (t, *J* = 7.0 Hz, 0.87H, H-14), 3.31–3.22 (m, 2H, H-12), 3.17 (s, 1.26H) and 2.94 (s, 1.59H, H-16), 1.97 (p, *J* = 6.9 Hz, 1.10H) and 1.89 (p, *J* = 6.8 Hz, 0.91H, H-13). **^{13}C NMR (101 MHz, DMSO)** δ 165.5 and 165.3 (C-17), 152.4 and 152.3 (C-3), 150.0 (C-1), 149.1 and 149.0 (C-5), 139.8 and 139.5 (C-19), 134.1 and 134.0 (C-2), 133.82 and 133.75 (C-20), 133.45 and 133.42 (C-7), 129.7, 129.3, 128.8, 128.5, 127.5 and 127.5 (C-8, C-6, C-21, and C-22), 124.2 and 124.1 (C-9), 123.9, 119.6 and 118.9 (C-18), 117.51 and 117.49 (C-10), 99.2 and 99.1 (C-2), 46.6 and 45.3 (C-14), 39.9 and 39.3 (C-12), 35.2 and 33.6 (C-16), 26.3 and 26.1 (C-13). **IR (cm^{-1})** 3419 (N-H stretch), 3107 (aromatic C-H stretch), 1645 (C=O), 1576 (C=C), 1380 (C-N stretch quinoline), 1140 (C-N stretch aliphatic). **HRMS(ESI-TOF+)**: *m/z* Calculated for $C_{22}H_{21}Cl_2N_3O$: 413.1062; found: 412.0987 (M-H). **mp**. 141–143 °C.

2.3.4. Synthesis of (E)-N-(3-((7-chloroquinolin-4-yl)amino)propyl)-3-(4-methoxyphenyl)-N-methylacrylamide (6c)

^{1}H NMR (400 MHz, DMSO) δ 8.40 (d, *J* = 5.4 Hz, 0.47H), 8.37 – 8.32 (m, 1.18H), 8.26 (d, *J* = 9.0 Hz, 0.44H, H-9), 7.83–7.76 (m, 1H, H-6), 7.65 (d, *J* = 8.3 Hz, 1H), 7.50 – 7.42 (m, 1.63H) and 7.41 – 7.32 (m, 1.94H, H-8, H-18 and NH), 7.28 (d, *J* = 8.3 Hz, 1H), 7.04 (d, *J* = 15.4 Hz, 0.44H), 6.95 (d, *J* = 8.3 Hz, 0.90H), 6.85 (d, *J* = 15.3 Hz, 0.62H, H-18), 6.68 (d, *J* = 8.3 Hz, 1H), 6.48 (d, *J* = 5.4 Hz, 1H, H-2), 3.78 (s, 1.28H) and 3.75 (s, 1.76H, H-24), 3.64 (t, *J* = 7.2 Hz, 1.27H) and 3.51 (t, *J* = 7.0 Hz, 0.90H, H-14), 3.33–.23 (m, 2H, H-12), 3.16 (s, 1.23H) and 2.94 (s, 1.71H, H-16), 2.04–.94 (m, 1H) and 1.95 – 1.84 (m, 1H, H-13). **^{13}C NMR (101 MHz, DMSO)** δ 166.0 and 165.7 (C-17), 160.4 and 160.2 (C-23), 152.0 (C-3), 150.1 (C-1), 149.1 (C-5), 141.1 and 140.8 (C-19), 133.5 (C-7), 129.7 and 129.2 (C-22), 127.8 (C-10), 127.52 (C-6), 127.47 (C-20), 124.2 and 124.0 (C-8 and C-9), 117.5 (C-1), 116.0 and 115.4 (C-18), 114.2 and 113.9 (C-21), 98.8 and 98.7 (C-2), 55.3 and 55.2 (C-24), 46.7 and 45.3 (C-14), 39.9 and 39.3 (C-12), 35.2 and 33.6 (C-16), 27.0 and 25.7 (C-13). **IR (cm^{-1})** 3441 (N-H stretch), 2993 (aromatic C-H stretch), 1642 (C=O), 1574 (C=C), 1248 (C-N stretch quinoline), 1139 (C-N stretch aliphatic). **HRMS(ESI-TOF+)**: *m/z* Calculated for $C_{23}H_{24}ClN_3O_2$: 409.1557; found: 408.1480 (M-H). **mp.** 130–132 °C.

2.4. Computational details

All the reaction species were optimized using the M06-2X density functional theory [33]. *Meta-GGA* functional is known for performing well towards optimization of reaction species and reaction barrier height energies [34,35]. The 6-311++G(d,p) basis set was selected because it consists of polarisation and diffuse functions, which are necessary to understand the properties of molecules and reaction mechanisms.

Calculations in solution were performed using five different solvents, benzene, Dichloromethane (DCM), methanol, Dimethyl sulfoxide (DMSO), and water. This selection was meant to assess the influence of the solvent on the stability of the compounds, in different solvents as a result of the difference in solvent polarity. The investigation in dichloromethane (DCM) and dimethyl sulfoxide (DMSO) media was meant to compare the results with experimental results for which these media were used. The study in benzene and water was meant to mimic the two extreme non-polar lipid mediums and polar aqueous mediums that can be found within the biological system. The solvation model based on density (SMD) was selected for utilization in the calculations [36].

The transition state structures were obtained by using the QST3 approach available in Gaussian program. Intrinsic reaction coordinate (IRC) calculations [37] were utilized to establish the connectivity between the reactant species and product species smoothly through the determined transition state structure. Vibrational frequency calculations were performed on the optimized species, using the same basis set as the basis set used to optimize the structure. The Gaussian software program [38] has been utilized throughout the study to optimize the structures. The output geometries are visualized by using the GausView Program.

3. Results and discussion

3.1. Synthesis and NMR analysis

To get a deeper understanding of the NMR behaviour of chloroquinoline-*N*-methyl acrylamides in terms of their conformation at room temperature, compounds were synthesized following our previously reported method [32] and an overview of the synthesis route to these analogues is depicted in Scheme 1. Following the synthesis, the interesting conformational arrangement of these compounds was studied using NMR spectroscopy.

Intermediate **2** was prepared by the aromatic nucleophilic substitution of chlorine under reflux for 8 h to afford the 4-amino-chloroquinoline. In a separate flask, a catalytic amount of DMF was added to a mixture of cinnamic acid with $SOCl_2$ in toluene at rt for 3 h to yield cinnamoyl chloride **4**. Later, intermediates **2** and **4** were conjugated in the presence of triethylamine as a base in DCM at rt for 18 h to afford **5** and **6** in poor to moderate yields of 34 % and 54 % respectively. The ^{1}H NMR spectrum for compound **5**, which depicted a total integration of 15 protons as expected, was compared with the newly synthesized compounds **6**.

Analysis of the proton signals for **5** showed a pentet at 1.87 ppm with a *J*-value of 6.8 Hz corresponding to the 'inner' methylene group of the linker and doublet of doublets integrated to 4 protons corresponding to the terminal methylene protons at 3.33 ppm. Additionally, both NH-protons overlapped with other methine protons of the quinoline and aromatic rings depicting multiplet at 8.28–8.24 ppm and 7.48–7.32 ppm respectively.

Compounds **6a-c** obtained where R = -CH_3 are unknown in the literature yet their structural features might be of biological interest; hence the reason their potential structural properties were studied. Surprisingly, the ^{1}H and ^{13}C NMR spectrum inspection showed complexity due to the substantial peak doubling as observed in Fig. 3.

Since precursor **2** has two secondary amine groups, the conjugation reaction could have occurred at either position. The less likely nucleophilic reaction could occur at the NH-(CQ)-C-1) to give **7**. Alternatively, the reaction could happen at NH-(-CH_3) to afford **6**. Lastly, it could take place at both amines and afford the mixture of two products, **6** and **7** (Scheme 1). To investigate this further, compound **6a** was reviewed and will be used as the referral compound for this reporting in all the experimental discussions. HRMS and FT-IR could not be used to determine the identity of the recovered product species because compounds **6** and **7** are structural isomers, however, HRMS confirmed the desired mass to be 378.1376. NMR spectroscopy was then used to investigate and confirm the recovered product because the technique can be used to distinguish between structural isomeric product species. HMBC experiment can be used to identify the position of *N*-methyl because the methyl protons would show a correlation to the C=O signal for **6** but not for compound **7**.

The analysis of the HMBC spectrum (Fig. S7) showed the correlation of the methyl signals confirming the recovery of compound **6**. With sufficient evidence that **6** was the formed compound, we hypothesized that in solution, it's likely that the compound exists as two rotamers because of restricted rotation around the C−N amide bond giving rise to the observed doubling of signals in both the ^{1}H and ^{13}C NMR spectrum [39].

Given the results we observed with these compounds, we also believed that the presence of the methyl group at *N*-15 was the sole contributor to the observed rotamers because similar compounds (**5**) devoid of the methyl group did not exhibit the doubling of ^{1}H and ^{13}C signals. The two rotamers gave rise to two distinct signals for all the resolved signals in the ^{1}H NMR spectrum as shown in Fig. 3 and Table 1. The highlighted methyl signals at 3.18 ppm and 2.96 ppm were the most resolved peaks used to determine the rotational barrier. Similarly, in the ^{13}C NMR spectrum, the methyl carbon groups exhibited double signals at 35.7 ppm and 34.1 ppm. Furthermore, at face value, some of the signals appear as though they are defined multiplets. For example, the two triplets at 3.67 (t, J = 7.2 Hz, 1.15H) and 3.53 (t, J = 7.0 Hz, 0.89H, H-14) can be mistaken for a doublet of triplets. However, the two triplets do not correlate to the same carbon signal in the HSQC of **6a** (Fig. 4), meaning they are separate triplets for each rotamer. Secondly, the integration of the doubling signals gives the desired total only when added together. The partial integration for the triplets is 1.15 and 0.89 which gives a total 2.04 for the desired number of expected signals. This is observed for all other doubling signals of **6a, 6b,** and **6c**.

Full assignment of the signals was achieved by using 2-dimensional COSY, HSQC, and HMBC in addition to the ^{1}H and ^{13}C NMR. The spectra are provided in the supporting documents. The distinction of the N-CH2 protons H-12 and H-14 was done by COSY and HMBC analysis. H-12 showed a COSY correlation to the NH proton in the aromatic ring whilst H-14 showed a correlation to the carbonyl C-17 signal in the HMBC spectrum. Doubling of signals was observed for almost all the ^{13}C NMR signals revealing that the two rotamers are stable and have different physical properties.

3.2. Variable temperature NMR analysis

To assess and confirm the presence of rotamer species, variable-temperature (V_T) NMR measurements were performed. Standard NMR analysis is performed at 27 °C hence to determine the coalescence temperature we analyzed the samples at 10 °C intervals. This technique is well established and has been used for studying restricted bond

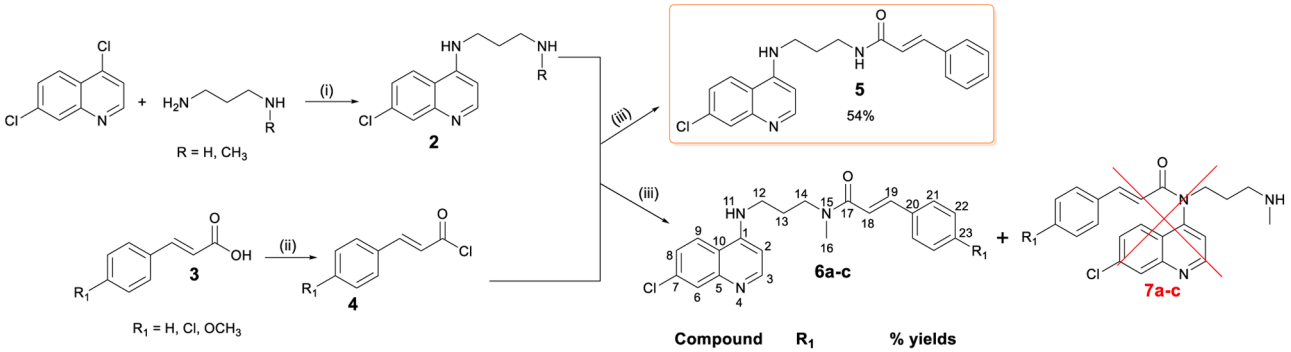

Compound	R_1	% yields
6a	H	43
6b	Cl	34
6c	OCH_3	53

Scheme 1. Synthetic route for preparation of compounds **5-6**. Reagents and conditions: (i) 165 °C, 8 h (ii) $SOCl_2$, toluene, 3 drops of DMF, RT, 3 h (iii) TEA, dry DCM, RT, 18 h.

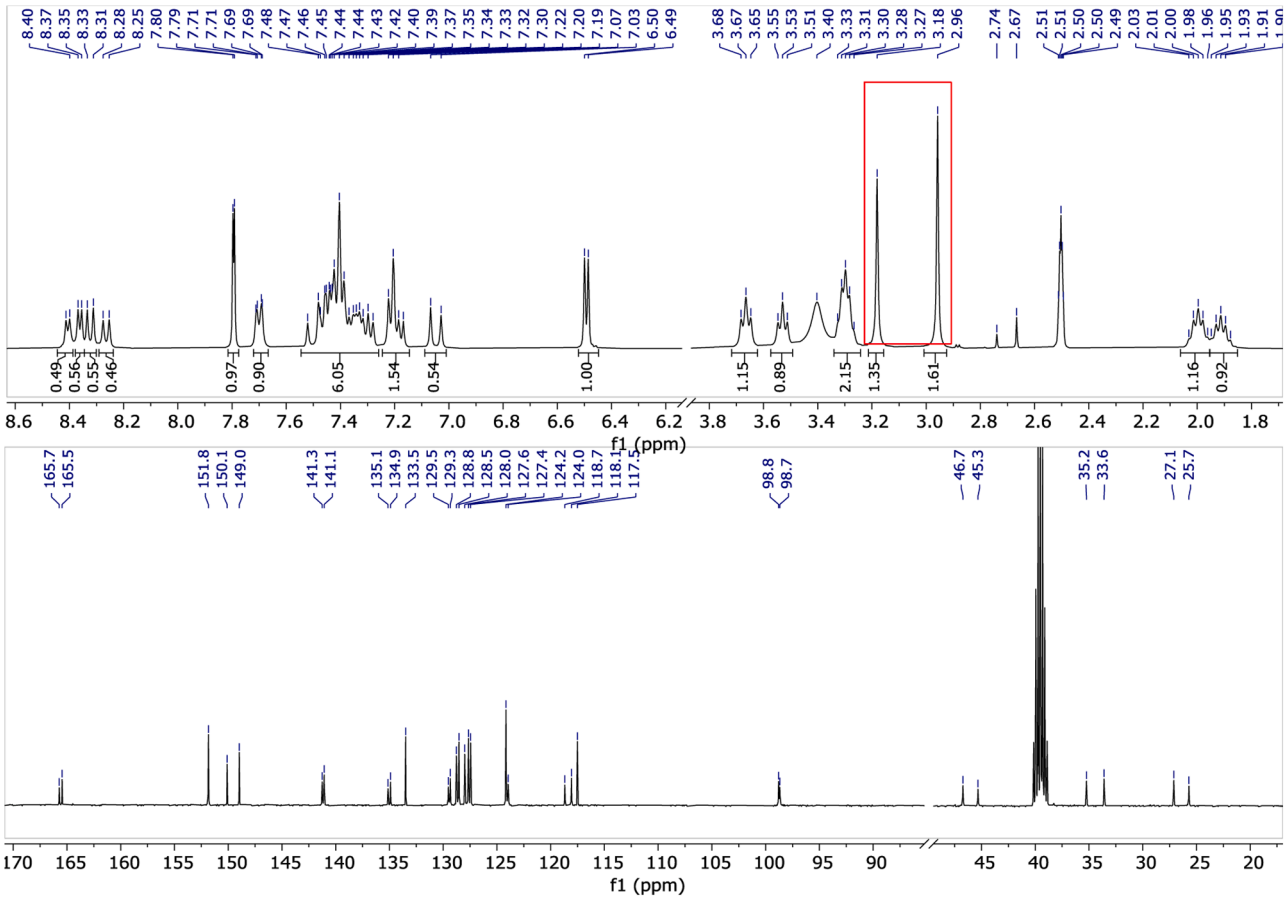

Fig. 3. ^{1}H and ^{13}C NMR spectra for compound **6a**.

Table 1
^{1} NMR and ^{13} NMR data of **6a** in DMSO.

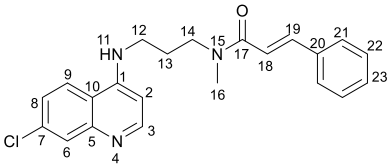

No	^{1}H NMR/ppm		^{13}C NMR/ppm	
2	δ = 6.49 (d, *J* = 5.5 Hz, 1H, H-2)		δ = 99.2	δ = 99.1
3	δ = 8.41 (d, *J* = 5.4 Hz, 0.49H)	δ = 8.36 (d, *J* = 5.4 Hz, 0.56H, H-3)	δ = 152.3	
9	δ = 8.32 (d, *J* = 9.0 Hz, 0.55H)	δ = 8.26 (d, *J* = 9.0 Hz, 0.46H, H-9)	δ = 124.2	δ = 124.0
14	syn rotamer δ = 3.67 (t, *J* = 7.2 Hz, 1.15H)	anti rotamer δ = 3.53 (t, *J* = 7.0 Hz, 0.89H, H-14)	syn rotamer δ = 47.2	anti rotamer δ = 45.8
13	syn rotamer δ = 2.00 (p, *J* = 7.0 Hz, 1.16H)	anti rotamer δ = 1.91 (p, *J* = 7.2 Hz, 0.92H, H-13)	syn rotamer δ = 27.6	anti rotamer δ = 26.2
12	3.34–3.324 (m, 2H, H-12)		40.6	40.2
16	anti rotamer δ = 3.18 (s, 1.35H, H-16)	syn rotamer δ = 2.96 (s, 1.61H, H-16)	anti rotamer δ = 35.7	syn rotamer δ = 34.1

rotation and determining rotational barrier energy [18,40].

For this procedure, the ^{1}H NMR experiments are performed at different temperatures whilst monitoring the coalescence of the rotameric signals. As the temperature of the sample mixture increases, more energy is provided which destabilizes the rotamers equilibrium resulting in a fast equilibrium and resultantly a coalescence of these signals is seen to occur and become indistinguishable by NMR as the doubling signals merge into one. The chemical shift difference between the rotamer signals decreases until the signals coalesce. Once the coalescence temperature, (T_c), has been determined, there are various techniques used to calculate the rotational barrier energy. One of the popular techniques employs the Eyring Eq. (1), which is used to determine the energy barrier ΔE, where R is the gas constant 8.314 JK^{-1}, the estimated coalescence temperature in Kelvins and Δν is the difference in chemical shift difference ($\delta_A - \delta_B$) of the individual rotamer signals at low temperature;

$$\Delta E = RT_c\left[22.96 + \ln\left(\frac{T_c}{\Delta\nu}\right)\right] \quad (1)$$

For this work, a set of ^{1}H NMR experiments were recorded over the temperature range of 27–90 °C and back to 27 °C (Fig. 5) in DMSO.

There were several signals we could have used to determine the rotational energy but for compound **6a** the methyl signals had the best baseline resolution hence their chemical shift was monitored as the temperature increased. Coalescence of the methylene linker signals was observed at 40 °C but it was approximately 60 °C for the methyl signals and this was the temperature used to calculate the rotational barrier energy. Using the Eyring equation it was determined to be 67.2 kJmol^{-1}. The greatest error in determining this value comes from accurately measuring T_c and from Fig. 5 T_c falls between 50 and 60 °C. Given this range, it is more accurate to report that the rotational energy barrier for compound **6a** is in the range of 65.1–67.2 kJmol^{-1}. Similar studies have been done on amide derivatives [31], where the rotational energy barrier of 3-[(*E*)-(dimethylamino) methylidene-1,1-dimethylurea was determined to be 68.6 kJmol^{-1} which is very similar to our

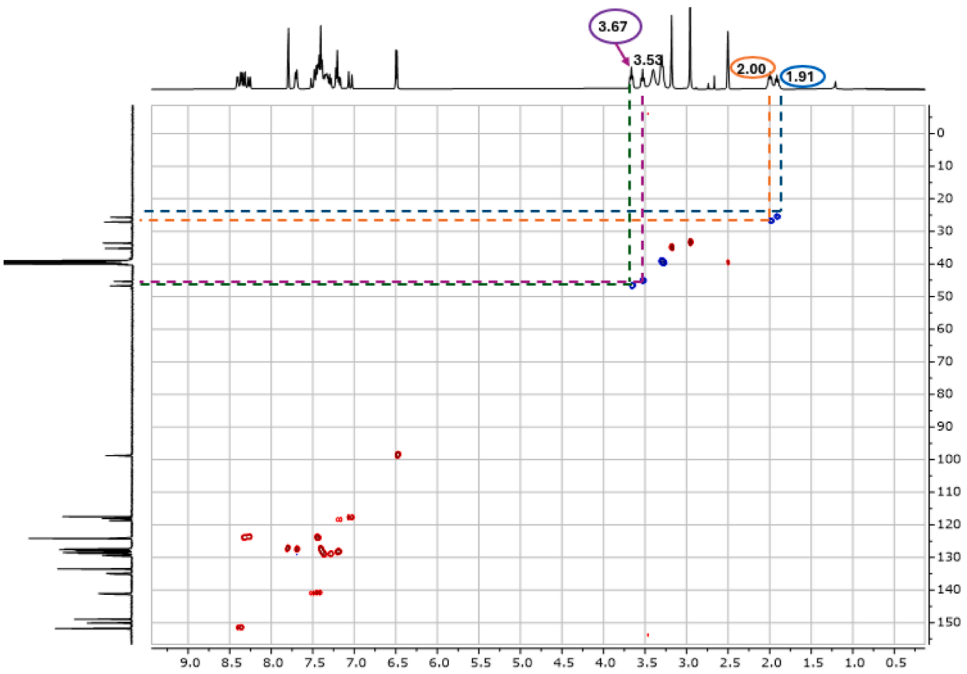

Fig. 4. The expanded HSQC spectrum of **6a** showing the direct correlation between protons and carbons.

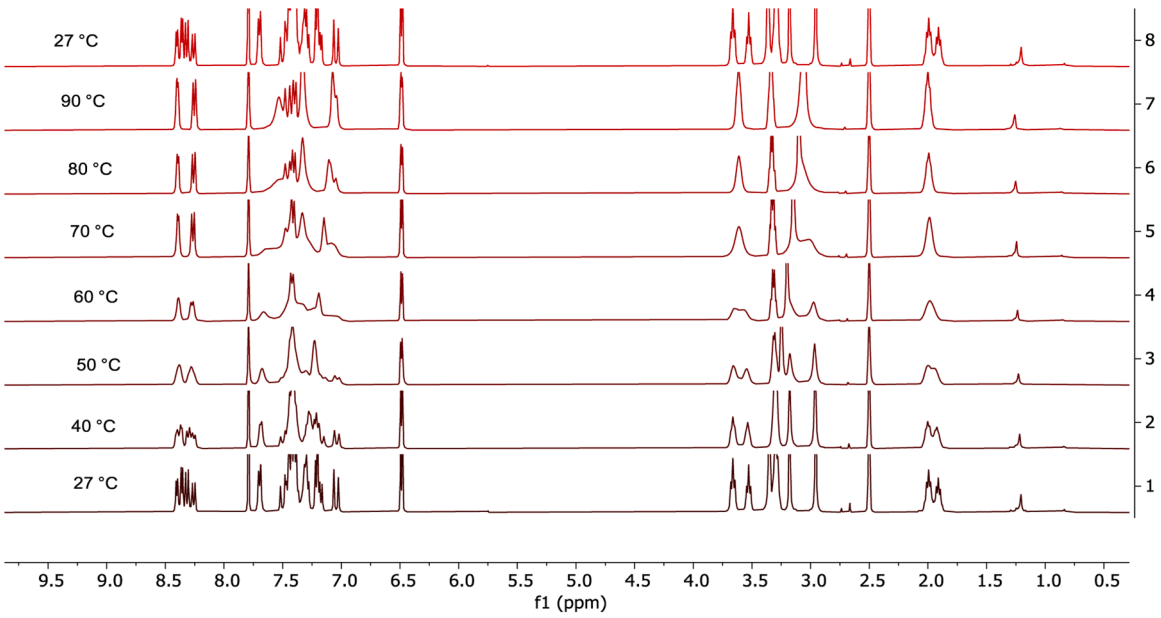

Fig. 5. Stacked plot ^{1}H NMR spectra of **6a** over 27–90 °C in DMSO.

experimentally determined value. The rotational energy barrier was determined to be the same for compounds **6b** and **6c**. The ^{1}H NMR spectrum obtained at 90 °C also helped to assign the signals as all the rotamers signals had coalesced (Fig. 6).

In addition to determining the rotational energy barrier between the two conformational isomers, we also performed low-temperature (0 °C) NOESY experiments to identify the *syn* and *anti*-signals. The experiments were carried out in MeOD and interestingly the ratio of the conformers decreased from 1:1.25 in DMSO to 1:1.1 in MeOD showing that the solvent affects the stability of the conformers at room temperature (Fig. 7). Pulsing either methyl signals during 1-D selective NOE at 27 °C was not selective on the NMR time scale and 0 °C was determined to be the optimal temperature before precipitation occurred. Loss of exchange of the signals was observed at this temperature. Irradiation of the major methyl signal at 3.04 ppm only generated NOE signals of the methylene linkage at 3.70 ppm and 2.08 ppm. However, irradiating the minor methyl signal at 3.21 ppm generates a NOE signal at 7.12 ppm (H-18) in addition to the methylene signals at 3.60 ppm and 1.96 ppm. Given these results, the major conformer is assigned to the *syn* configuration whilst the minor conformer is assigned to the *anti* configuration.

3.3. *Mechanism of formation for **6a-c** species*

The mechanism of the formation of **6a-c**, each from its monomer structures **2** and **4**, has also been investigated to measure the barrier height for its formation. The optimized reaction species (reactants,

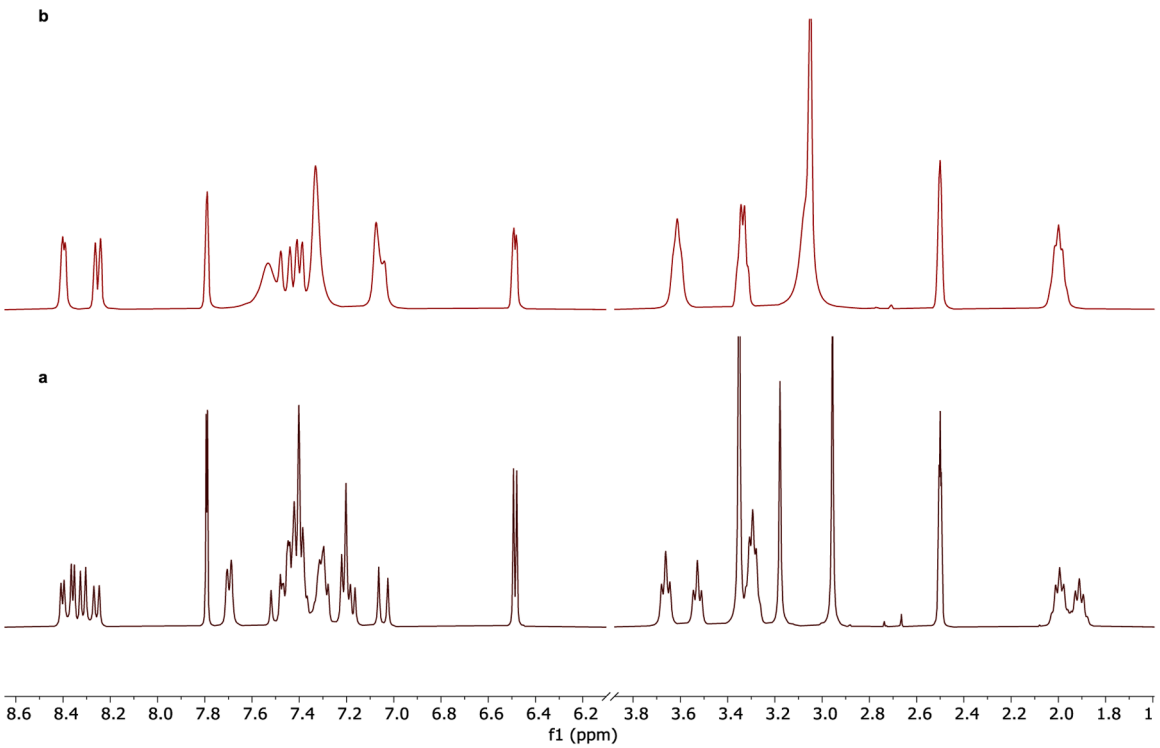

Fig. 6. Temperature-dependent NMR spectra of **6a** in DMSO at (a) 27 °C, (b) 90 °C.

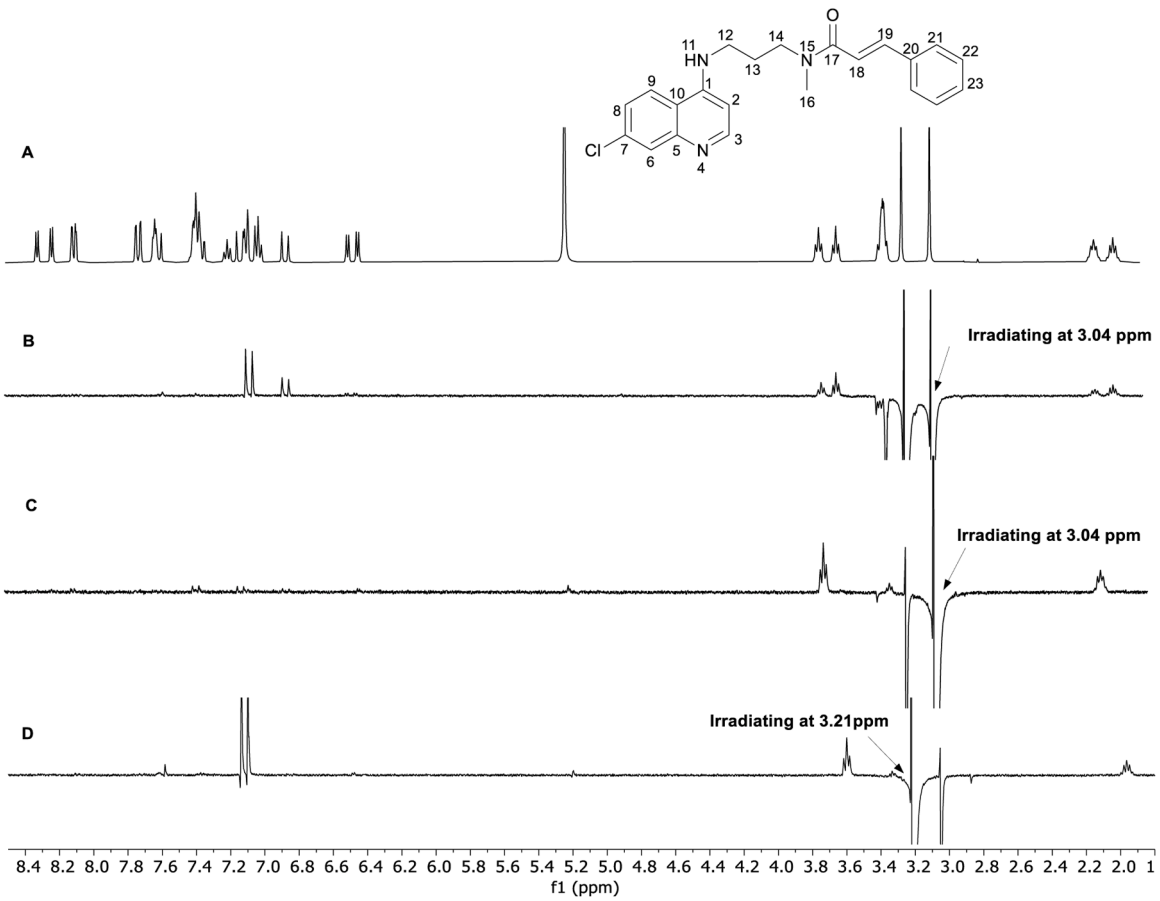

Fig. 7. (A) ^{1}H NMR for **6C** in MeOD at 27 °C, (B) Selective NOE of methyl at 3.04 ppm at 27 °C, (C) Selective NOE of methyl at 3.04 ppm at 0 °C, (D) Selective NOE of methyl at 3.21 ppm at 0 °C

transition states, and product species) are shown in Fig. 8. The energy versus reaction coordinate profile for the **6a** reaction species is shown in Fig. 9; Table 2 reports all the relative electronic energy and Gibbs free energy values for all the reactions studied. It is evident that in each case, the reaction may proceed through the formation of the reactant complex. This is because the energy of RC is lower than the sum of the energy of the isolated reactant species. The reactant species are stabilized by possible intermolecular interactions involving the interacting molecules. The **6a, 6b,** and **6c** reactant complex species are stabilized by the presence of hydrogen bonds between the amide group at N15 and the *keto* group at C17.

The transition state is characterized by the close approach of N15 and C17 as well as the expulsion of the chloride ion. The N15−C17 has a bond distance (Å) of 1.808, 1.818, and 1.806 in the transition structures of **6a, 6b**, and **6c**, respectively. N15−C17 amide bond distances in the given TS are longer than the standard covalent N−C amide bond length of 1.334 Å in secondary amides [41]. The N15−C17 bond in **6a, 6b**, and **6c** species has a bond vibration frequency value (cm^{-1}) of 127, 126, and 132, respectively. The product complex species consists of the chloroquine-cinnamic acid conjugate product species interacting with the HCl by-product species.

The barrier height for the formation of the **6a, 6b,** and **6c** product species is about 12 − 13 kcal/mol. The reaction Gibbs free energy for the reactions has a negative value, which indicates that the reaction is

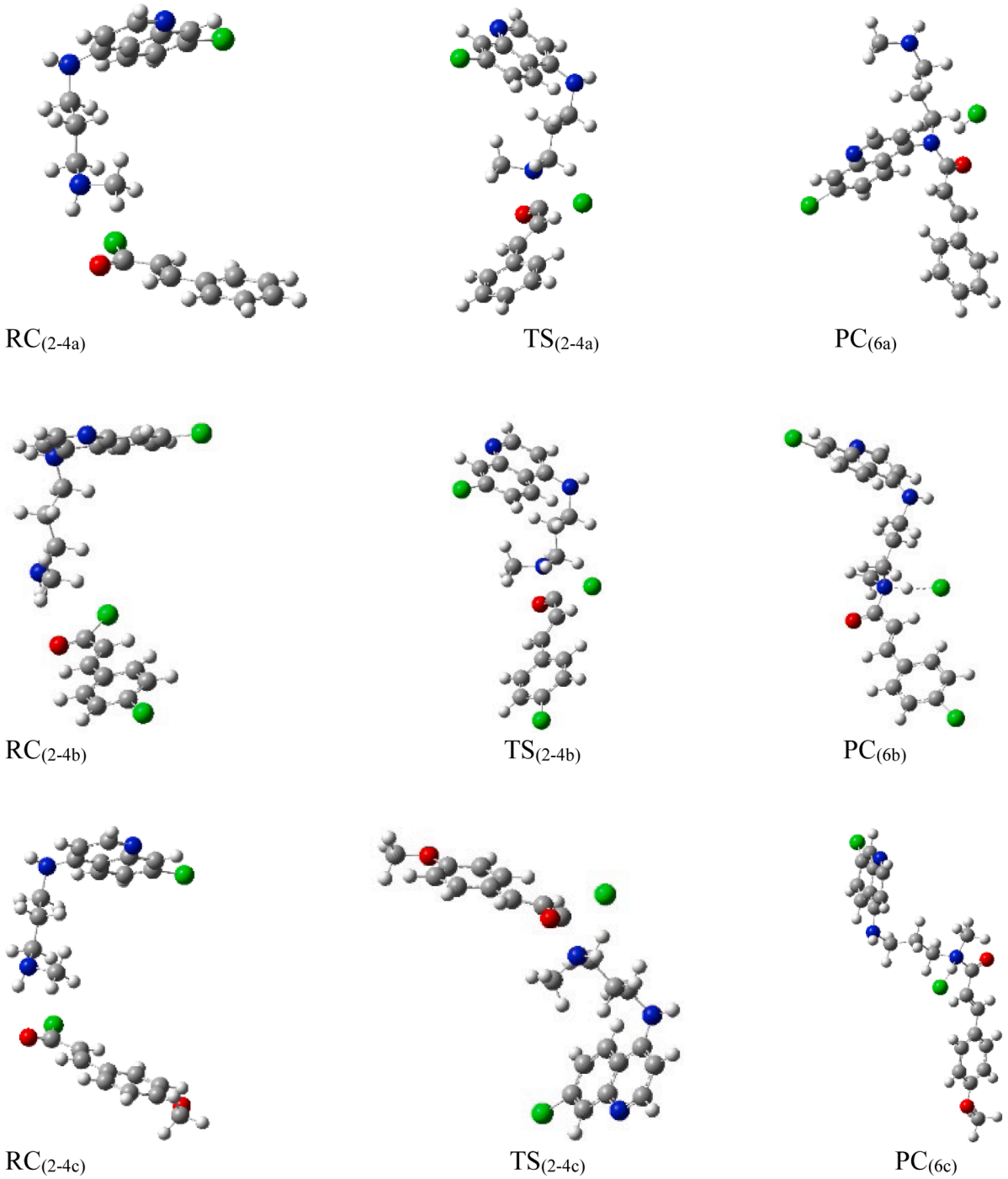

Fig. 8. Optimized reactant complex (RC), transition state (TS), and product complex (PC) reaction species for the formation of **6a, 6b**, and **6c**.

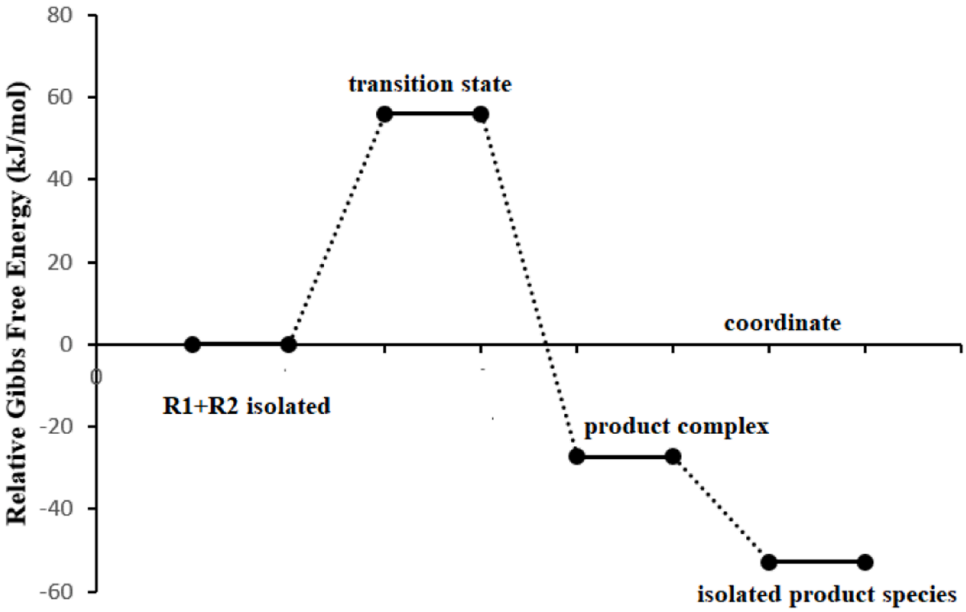

Fig. 9. Energy (relative Gibbs free energy) versus coordinate for the reaction involving structure **2** (R1) and **4** (R2) shown in Fig. 7 with R = H. The reaction is performed at room temperature using the M06−2X/ 6-311++G(d,p) method. A similar pattern was obtained when R = Cl and OCH_3.

Table 2
Relative electronic energy (ΔE, kcal/mol) and relative free energy (ΔG, kcal/mol) values for the species involved in the formation of ***6a-c***.

Structures	Relative energy (ΔE, kcal/mol)	Relative free energy (ΔG, kcal/mol)
$(2 + 4a)_{iso}$	0.0	0.0
$RC_{(2\text{-}4a)}$	−20.3	21.1
$TS_{(2\text{-}4a)}$	2.8	56.1
$PC_{(6a)}$	−77.9	−27.2
P iso	−67.4	−52.9
$(2 + 4b)_{iso}$	0.0	0.0
$RC_{(2\text{-}4b)}$	−19.7	30.9
$TS_{(2\text{-}4b)}$	1.6	52.8
$PC_{(6b)}$	−77.6	−25.8
P iso	−68.9	−55.6
$(2 + 4c)_{iso}$	0.0	0.0
$RC_{(2\text{-}4c)}$	−21.1	18.7
$TS_{(2\text{-}4c)}$	6.1	57.1
$PC_{(6c)}$	−76.7	−25.3
P iso	−63.7	−48.9

thermodynamically preferred towards the formation of the product species.

3.4. Stability of the rotamers for the studied acrylamides

The product species **6a-c** and **7a-c** have various rotatable single bonds, allowing for the existence of several conformers for each structure. The stability of the different conformers for each structure is influenced by the steric hindrance emanating from close proximity of the various substituent groups, the presence of non-covalent interactions such as hydrogen bonding and π···C-H interactions as well as the *anti-* and *syn* arrangement associated with the imide C−N group. The optimized structures of the rotamers are shown in Fig. 10.

Among the **6a-c** structures, the preferred structures are those that form intermolecular hydrogen bond involving the C3−H group and the O17 atom for the results *in vacuo*. In the presence of the solvent, however, this intermolecular interaction appears to be weakened as O17 interacts with solvent molecules. The linear orientation of the aliphatic chain is preferred to the bending orientation, except when the bending of the chain would result in the formation of intermolecular hydrogen bond. The influence of the imide C−N bond rotation on the stability of the conformers was studied by also taking into account **5a** to compare the effect of the methylation at the amide group, which differentiates tertiary and secondary amides. The rotamer for which the C-N-C17=O17 torsion angle is near zero corresponds to an *anti-* while the rotamer for which the C-N-C17=O17 torsion angle is near 180° represents a *syn*-one. The relative energy of the *anti-*, and *syn-* species are reported in Table 3. Fig. 11 shows the rotational barrier for the formation of the *syn*-rotamer from the *anti*-rotamer for the results *in vacuo* of the **5a, 6a, 6b,** and **6c**. The formation of the *syn*-rotamer from the *anti*− rotamer or vice versa generally goes through the formation of either the TS_{anti} or the TS_{syn} transition state structures [26]. Previous studies on amides and carbamates have identified that in most cases, the TS_{anti} is more preferred to the TS_{syn} transition state structure [42–44]. For this reason, we have approached the investigation of the *anti*↔*syn* rotamer interconversion of the herein synthesised amide derivatives through the formation of the TS_{anti} structure. The barrier height (kJ/mol) found in each *anti*↔ *syn* rotamer interconversion case is 66.6 for **6a**, 65.2 for **6b,** and 59.4 for **6c**. These prove that the NMR and computational methods are in excellent agreement with one another. Following the calculations performed *in vacuo*, the experimental values are slightly larger due to solvent and other interactive molecular effects.

The formation of the *syn*− rotamer from the *anti*− rotamer in the case of **5a** has a much higher barrier height of 78.8 kJ/mol. Moreover, the *syn* rotamer stability to the *anti*− in the case of **6a-c** structures is ≈ 1 kcal/mol, indicating that both rotamers can be considered to co-exist in nature. However, in the case of **5a**, only the **anti-**rotamer can be considered to be stable, as the Boltzmann distribution (%) for this rotamer is 99.7 *in vacuo*, 98.8 in DCM, 97.5 in methanol, 95.4 in DMSO and 82.3 % water solution. The stability of the syn-rotamer increases with the increase in solvent polarity. In other words, the secondary amides of the investigated structures are likely to favour the formation of only the *anti*− rotamers in non-polar medium. However, tertiary amides of the studied acrylamides (structures **6a-c**) are likely to exist in the mixture of both *anti*− and *syn*− rotamers, since the two structures are close to each other in energy. the stability of one conformer with respect to the other conformer is influenced by the medium in which the investigation is carried out; for structure **6a** and **6b**, the *syn*−rotamer species is more stable than the *anti*−rotamer species in all media except in DCM, for

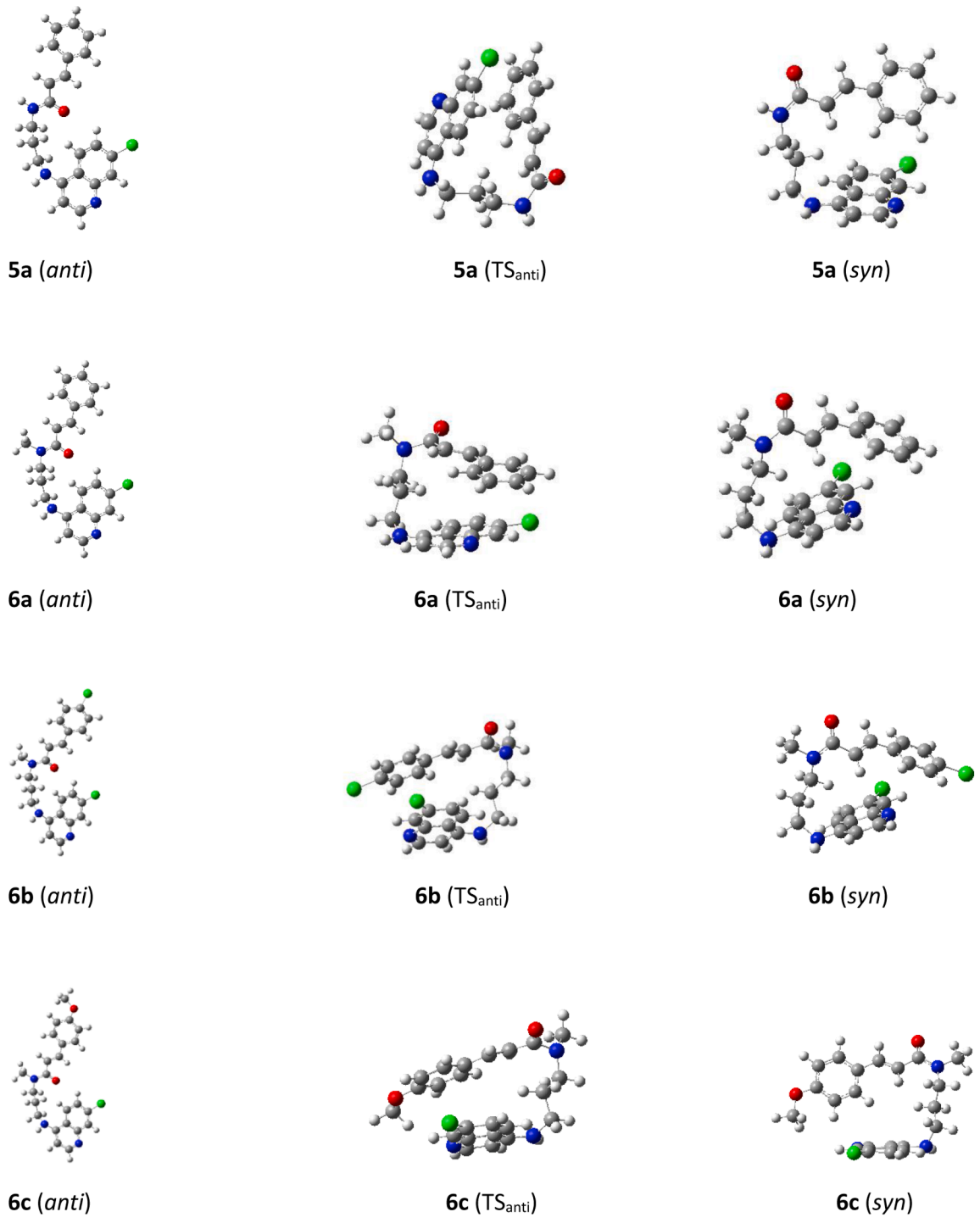

Fig. 10. M06−2X/ 6-31++G(d,p) optimized geometries for the interconversion of the *anti*-rotamer to form the *syn*-rotamer through transition state TS_{anti} for the studied compounds

structure **6c**, the *syn*−rotamer species is more stable than the *anti*-−rotamer species in all media. These results collaborate well with our experimental results reported herein. From a thermodynamic Gibbs free energy data, it is reasonable to infer that among the **6a-c** structures, the *anti*− rotamer evolves from the syn− rotamer, since the energy change in such respective would correspond to a negative ΔG.

The stability of the conformers of structures **7a-c** is largely influenced by the steric hindrances associated with the cinnamoyl and the aliphatic $CH_2CH_2CH_2NH(CH_3)$ substitute groups at N11; it is evident that the most stable conformers correspond to cases in which the two substituent groups are far apart, thereby decreasing the steric hindrance between them. Table 4 provides a comparison of the stability between corresponding lowest-energy conformers of **6a-c** and 7a-c. The outcome suggests that **6a, 6b,** and **6c** are significantly stable in comparison to **7a, 7b,** and **7c** respectively; indicating that the structure that is most likely to form is **6** rather than **7**. These results are consistent with our experimental results, which point to the formation of the NH-($-CH_3$) to afford **6**.

Table 3
Relative energy (kJ/mol) and relative free energy (kJ/mol) for the *anti*– and *syn*– rotamers of structures 5a and 6a-c calculated in different media using M06-2X/6-31++G(d,p) calculation approach.

structures	anti/syn relative energy (ΔE, kJ/mol)					anti/syn relative free energy (ΔG, kJ/mol)				
	benzene	DCM	methanol	DMSO	water	benzene	DCM	methanol	DMSO	water
5a-ant	0.0	0.0	0.0	0.0	0.0	0.0	0.0	0.0	0.0	0.0
5a-syn	14.4	10.9	9.0	7.5	3.8	21.1	17.8	18.8	18.0	13.3
6a-ant	0.0	0.0	0.0	0.0	0.0	0.0	0.0	0.0	0.0	0.0
6a-syn	-1.7	4.0	-2.5	-2.4	-2.6	9.1	12.9	-0.3	11.3	6.6
6b-ant	0.0	0.0	0.0	0.0	0.0	0.0	0.0	0.0	0.0	0.0
6b-syn	-3.3	4.0	-5.2	-1.1	-8.9	14.1	11.8	0.8	11.0	-1.8
6a-ant	0.0	0.0	0.0	0.0	0.0	0.0	0.0	0.0	0.0	0.0
6b-syn	-8.4	-2.8	-3.5	-8.3	-8.3	-2.7	3.7	5.3	-4.0	-3.4

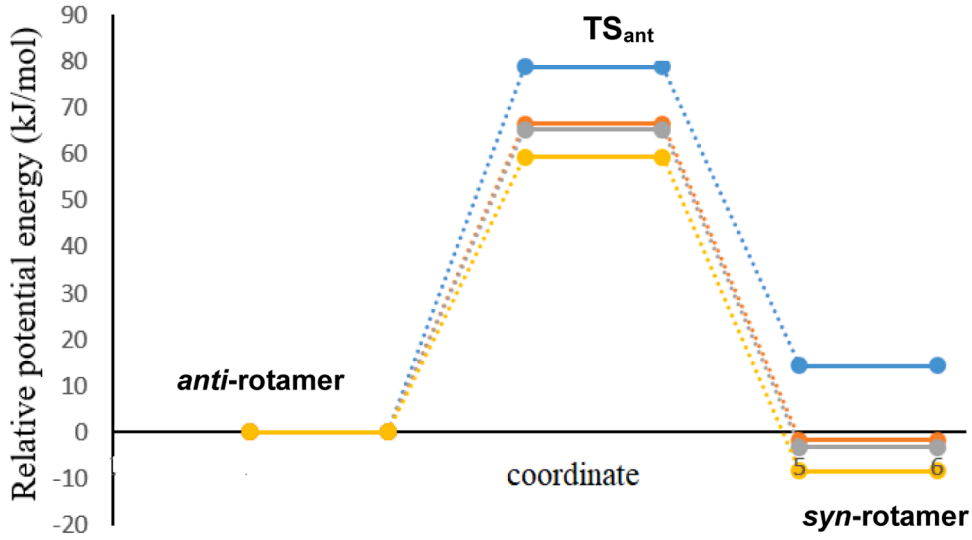

Fig. 11. Energy versus coordinate for the interconversion from *anti* rotamer to *syn* rotamer for **5a** (blue colour), **6a** (orange colour), **6b** (grey colour), and **6c** (yellow colour) *in vacuo*. Results were obtained using M06−2X/ 6-31++G(d,p) method.

Table 4
Relative energies (kcal/mol) and selected torsion angle (°) in different media for the structures **6a-c** and **7a-c**; results obtained using M06−2X/6-311++G(d,p) calculation method.

Structure	Torsion angle [a]	Torsion angle value (°) in different media						Relative energy (kcal/mol)					
		vacuum	benzene	DCM	methanol	DMSO	water	*in vacuo*	benzene	DCM	methanol	DMSO	water
6a	C14-N15-C17-O17	0.8	-0.2	1.4	1.2	1.5	5.5	0.000	0.000	0.000	0.000	0.000	0.000
7a	C1-N11-C17-O17	-161.9	-164.6	-165.2	-166.5	-165.1	-164.3	2.961	3.660	5.207	5.543	5.534	5.271
6b	C14-N15-C17-O17	0.3	0.8	2.3	0.5	1.9	4.58	0.000	0.000	0.000	0.000	0.000	0.000
7b	C1-N11-C17-O17	-162.6	-164.7	-165.8	-166.2	-165.1	-164.5	2.941	3.833	4,721	5.646	5.058	5.528
6c	C14-N15-C17-O17	0.60	0.4	1.3	1.02	2.1	6.4	0.000	0.000	0.000	0.000	0.000	0.000
7c	C1-N11-C17-O17	-162.5	-164.7	-165.8	-166.4	-165.0	-164.5	2.705	3.641	5.016	5.545	5.419	5.441

[a]the oxygen atom on C17 is also given the number 17.

4. Conclusions

The preparation and analysis of new cinnamoyl-chloroquinoline derivatives was conducted. Using the known synthetic methods, and after thorough purification by silica gel column chromatography and crystallization, all the acrylamide compounds, **6a-c** were obtained in moderate yields and purities. For the first time, these biologically important compounds' stereodynamic behaviour was studied by dynamics and multinuclear ^{1}H, ^{13}C spectroscopy in DMSO-d_6 solution to determine the barrier to their internal rotation. These barriers were also determined computationally, and both methods were found to be in excellent agreement. Owing to the NMR analysis, the rotational conformers resulting from the tertiary amide were recognized using VT NMR experiments which proved that at higher temperatures (60 °C), signals of all rotamers coalesced.

The results of DFT investigations calculations have confirmed our experimental findings that **6a-c** are preferred products to **7a-c** results for the synthesis of quinoline-cinnamic hybrid analogues using different amino-amide linkers. Among the rotamers of **6a-c**, it is evident that both the *anti*– and *syn*– rotamers co-exist due to their minimal energy

difference. Finally, a comparison of **5a** and **6a** structures suggests that the presence of the methyl group at the amide nitrogen, N(CH_3) could account for the fact that both the *anti*− and the *syn*− rotamers co-exist among the tertiary amide derivatives and that the *syn*− rotamer is the most stable one as confirmed by the experimental NMR (NOE) results. This is because, amidst the secondary amide derivatives such as **5a**, only the *anti*− rotamer is significantly stable.

Supporting information

Spectra data for all the compounds are provided. This material is available as supporting information.

CRediT authorship contribution statement

Mpelegeng V. Bvumbi: Writing – review & editing, Writing – original draft, Validation, Supervision, Resources, Project administration, Methodology, Investigation, Funding acquisition, Formal analysis, Conceptualization. **Memory Zimuwandeyi:** Writing – review & editing, Resources, Formal analysis, Data curation. **Anza I. Nemudzivhadi:** Writing – review & editing, Investigation, Formal analysis, Data curation. **Mwadham M. Kabanda:** Writing – review & editing, Writing – original draft, Validation, Software, Data curation.

Declaration of competing interest

The authors declare a conflict of no interest.

Acknowledgments

The authors thank the University of Venda's RPC and National Research Foundation (Thuthuka Grant no: TTK220407250) for funding this project. The CSIR Centre for High-Performance Computing (CHPC) in South Africa is also acknowledged for providing computational resources.

Supplementary materials

Supplementary material associated with this article can be found, in the online version, at doi:10.1016/j.molstruc.2025.141943.

Data availability

Data will be made available on request.

References

[1] V.D.P. Gupta, P. Datta, Next-generation strategy for treating drug-resistant bacteria: antibiotic hybrids, Indian J. Med. Res. 149 (2019) 97–106, https://doi.org/10.4103/ijmr.IJMR.
[2] D.S. Walsh, DS. Walsh, C. Eamsila, T. Sasiprapha, S. Sangkharomya, P. Khaewsathien, P. Supakalin, D.B. Tang, P. Jarasrumgsichol, C. Cherdchu, M. D. Edstein, K.H. Rieckmann, T.G. Brewer, Efficacy of monthly tafenoquine for prophylaxis of *Plasmodium vivax* and multidrug-resistant *P. falciparum* malaria, J. Infect. Dis. 190 (2004) 1456–1463, https://doi.org/10.1086/424468.
[3] D.S. Barnett, R.K. Guy, Antimalarials in development in 2014, Chem. Rev. 114 (2014) 11221–11241, https://doi.org/10.1021/cr500543f.
[4] T. Fröhlich, C. Reiter, M.M. Ibrahim, J. Beutel, C. Hutterer, I. Zeitträger, H. Bahsi, M. Leidenberger, O. Friedrich, B. Kappes, T. Efferth, M. Marschall, S.B. Tsogoeva, Synthesis of novel hybrids of quinazoline and artemisinin with high activities against *plasmodium falciparum*, human cytomegalovirus, and leukemia cells, ACS Omega 2 (2017) 2422–2431, https://doi.org/10.1021/acsomega.7b00310.
[5] B. Pérez, C. Teixeira, J. Gut, P.J. Rosenthal, J.R.B. Gomes, P. Gomes, Cinnamic acid/chloroquinoline conjugates as potent agents against chloroquine-resistant plasmodium falciparum, ChemMedChem 7 (2012) (2012) 1537–1540, https://doi.org/10.1002/cmdc.201200257.
[6] B.C. Pérez, C. Teixeira, M. Figueiras, J. Gut, P.J. Rosenthal, J.R.B. Gomes, P. Gomes, Novel cinnamic acid/4-aminoquinoline conjugates bearing non-proteinogenic amino acids: towards the development of potential dual-action antimalarials, Eur. J. Med. Chem 54 (2012) 887–899, https://doi.org/10.1016/j.ejmech.2012.05.022.
[7] N.K. Davydova, O.V. Sinitsyna, V.N. Sergeev, I. Perevyazko, E.E. Laukhina, Towards DNA sensing polymers: interaction between acrylamide/3-(: N, N -dimethylaminopropyl)-acrylamide and DNA phage λ at various N/P ratios, RSC Adv. 6 (2016) 58212–58217, https://doi.org/10.1039/c6ra11231e.
[8] P. Singhsa, D. Diaz-Dussan, H. Manuspiya, R. Narain, Well-defined cationic N-[3-(Dimethylamino)propyl]methacrylamide hydrochloride-based (Co)polymers for siRNA delivery, Biomacromolecules 19 (2018) 209–221, https://doi.org/10.1021/acs.biomac.7b01475.
[9] S. Tsukagoshi, N. Ototake, Y. Ohnishi, M. Shimizu, O. Kitagawa, Unique structural properties of 2,4,6-tri-tert-butylanilide: isomerization and switching between separable amide rotamers through the reaction of anilide enolates, Chem. A Eur. J. 19 (2013) 6845–6850, https://doi.org/10.1002/chem.201300201.
[10] J.S. Laursen, J. Engel-Andreasen, P. Fristrup, P. Harris, C.A. Olsen, Cis -trans amide bond rotamers in β-peptoids and peptoids: evaluation of stereoelectronic effects in backbone and side chains, J. Am. Chem. Soc 135 (2013) 2835–2844, https://doi.org/10.1021/ja312532x.
[11] S.J. Shandler, M.V. Shapovalov, R.L. Dunbrack, W.F. Degrado, Development of a rotamer library for use in β-peptide foldamer computational design, J. Am. Chem. Soc. 132 (2010) 7312–7320, https://doi.org/10.1021/ja906700x.
[12] L. Cipolla, C. Airoldi, D. Bini, M. Gregori, F. Marcelo, J. Jiménez-Barbero, F. Nicotra, Fructose-based proline analogues: exploring the prolyl trans/cis-amide rotamer population in model peptides, Eur. J. Org. Chem. 1 (2011) 128–136, https://doi.org/10.1002/ejoc.201000983.
[13] T. Lanyon-Hogg, M. Ritzefeld, N. Masumoto, A.I. Magee, H.S. Rzepa, E.W. Tate, Modulation of amide bond rotamers in 5-acyl-6,7-dihydrothieno[3,2-c]pyridines, J. Org. Chem. 80 (9) (2015) 4370–4377, https://doi.org/10.1021/acs.joc.5b00205.
[14] W.D. Phillips, Restricted rotation in amides as evidenced by nuclear magnetic resonance, J. Chem. Phys. 23 (1955) 1363–1364, https://doi.org/10.1063/1.1742298.
[15] Y. Shvo, E.C. Taylor, K. Mislow, M. Raban, Chemical shift nonequivalence of diastereotopic protons due to restricted rotation around aryl-nitrogen bonds in substituted amides, J. Am. Chem. Soc. 89 (1967) 4910–4917, https://doi.org/10.1021/ja00995a015.
[16] E.R. Johnston, R. Fortt, J.C. Barborak, Correlated rotation in a conformationally restricted amide, Magn. Reson. Chem. 38 (2000) 932–936, https://doi.org/10.1002/1097-458X(200011)38:11<932::AID-MRC752>3.0.CO;2-6.
[17] V.V. Krishnan, S. Vazquez, K. Maitra, S. Maitra, Restricted amide rotation with steric hindrance induced multiple conformations, Chem. Phys. Lett 689 (2017) 148–151, https://doi.org/10.1016/j.cplett.2017.10.013.
[18] M.T. Huggins, T. Kesharwani, J. Buttrick, C. Nicholson, Variable temperature NMR experiment studying restricted bond rotation, J. Chem. Educ. 97 (2020) 1425–1429, https://doi.org/10.1021/acs.jchemed.0c00057.
[19] E.A. Basso, P.R. Oliveira, F. Wiectzycoski, R.M. Pontes, B.C. Fiorin, NMR and theoretical study of the (C=O)-N rotational barrier in the isomers cis- and trans- 2-N,N-dimethylaminecyclohexyl 1-N′,N′- dimethylcarbamate, J. Mol. Struct. 753 (2005) 139–146, https://doi.org/10.1016/j.molstruc.2005.06.001.
[20] R.J. Smith, D.H. Williams, K. James, Analysis of the rotational motions of the guanidino group in arginine, J. Chem. Soc. Chem. Commun. 11 (1989) 682–683, https://doi.org/10.1039/C39890000682.
[21] B.J. Wik, M. Lersch, A. Krivokapic, M. Tilset, Adding a new dimension to the investigation of platinum-mediated arene C-H activation reactions using 2D NMR exchange spectroscopy. Dynamics of Pt(II) phenyl/benzene site exchange, J. Am. Chem. Soc. 128 (2006) (2006) 2682–2696, https://doi.org/10.1021/ja056694z.
[22] A. Anand, A.D. Roy, R. Chakrabarty, A.K. Saxena, R. Roy, Investigation of the barrier to the rotation of carbamate and amide C-N bonds in antidepressant (6aR*,11bS*)-7-[carbobenzyloxy-l-alanyl]-2-[(4-methylphenyl)sulfonyl]-1,2,3,4,6,6a,7,11b,2,12a(S)-decahydropyrazino[2′,1′:6,1]pyrido[3,4-b]indole by dynamic NM, Tetrahedron 63 (2007) 5236–5243, https://doi.org/10.1016/j.tet.2007.03.171.
[23] C.H. Bushweller, J.W. O'Neil, M.H. Halford, F.H. Bissett, Activation parameters for conformational isomerism in an N-acetylpyrrolidine by total nuclear magnetic resonance line shape analysis and direct thermal stereomutation, J. Chem. Soc. D 225 (1971) 1251–1252, https://doi.org/10.1039/C29700001251.
[24] S.A. Matchett, G. Zhang, D. Frattarelli, Measurement of olefin bond rotation barriers in a series of vinylaniline complexes of the cyclopentadienyliron(II) dicarbonyl cation and their correlation to metal-olefin bond asymmetry, Organometallics 23 (2004) 5440–5449, https://doi.org/10.1021/om040092r.
[25] M.Z. Sadvakassova, A.I. Khlebnikov, A.A. Bakibaev, O.A. Kotelnikov, R. Sh. Erkassov, M.A. Yelubay, M.A. Issabayeva, Rotational barriers in N-benzhydrylformamides : an NMR and DFT study, Molecules 28 (2023) 535.
[26] M. Horwath, V. Benin, C−N bond rotation and E-Z isomerism in some N-benzyl-N-methylcarbamoyl chlorides: A DFT study, J. Mol. Struct. Theochem. 850 (2008) 105–110, https://doi.org/10.1016/j.theochem.2007.10.028.
[27] M. Kissane, M. Murphy, E. O'Brien, J. Chopra, L. Murphy, S.G. Collins, S. E. Lawrence, A.R. Maguire, Addition-substitution reactions of 2-thio-3-chloroacrylamides with carbon, nitrogen, oxygen, sulfur and selenium nucleophiles, Org. Biomol. Chem. 9 (2011) 2452–2472, https://doi.org/10.1039/c0ob00805b.
[28] J. Mandel, X. Pan, E. Ben Hay, S.J. Geib, C.S. Wilcox, D.P. Curran, Rotational isomers of N-methyl-N-arylacetamides and their derived enolates: implications for asymmetric Hartwig oxindole cyclizations, J. Org. Chem. 78 (2013) 4083–4089, https://doi.org/10.1021/jo400385t.
[29] S. Song. S. Song, T. Hyodo, H. Ikeda, K.A.L. Vu, Y. Tang, E.S. Chan, Y. Otani, S. Inagaki, K. Yamaguchi, T. Ohwada, Contribution of solvents to geometrical preference in the Z/E equilibrium of N-phenylthioacetamide, J. Org. Chem. 87 (2022) 1641–1660, https://doi.org/10.1021/acs.joc.1c00801.

[30] L.I. Larina, A.I. Albanov, S.N. Zelinskiy, V.V. Annenkov, I.L. Rusakova, Acrylamide derivatives: A dynamic nuclear magnetic resonance study, Magn. Reson. Chem. 61 (2023) 277–283, https://doi.org/10.1002/mrc.5331.
[31] N.G. Vassilev, I.C. Ivanov, A small change in structure, a big change in flexibility, Molecules 28 (2023) 1–13.
[32] M.M. Kabanda, A.I. Nemudzivhadi, M.V. Bvumbi, N.E. Madala, Rationalizing the formation of quasi-molecular anions due to tautomerization of chloroquine-cinnamide hybrid molecule during analysis by electrospray ionization (ESI) – mass spectrometry (MS) and through density functional theory (DFT) calculations, J. Mol. Struct. 1291 (2023) 136014, https://doi.org/10.1016/j.molstruc.2023.136014.
[33] Y. Zhao, D.G. Truhlar, The M06 suite of density functionals for main group thermochemistry, thermochemical kinetics, noncovalent interactions, excited states, and transition elements: two new functionals and systematic testing of four M06-class functionals and 12 other functions, Theor. Chem. Acc. 120 (2008) (2008) 215–241, https://doi.org/10.1007/s00214-007-0310-x.
[34] M.M. Kabanda, I. Bahadur, A DFT and MP2 mechanistic and kinetic study on hypohalogenation reaction of cysteine and N-acetylcysteine in aqueous solution, J. Mol. Liq. 349 (2022) 118191, https://doi.org/10.1016/j.molliq.2021.118191.
[35] M.M. Kabanda, I. Bahadur, P. Singh, Antioxidant and anticancer properties of plant-based bioactive flavonoids cardamonin and alpinetin: A theoretical insight from •OOH antiradical and Cu (II) chelation mechanisms, J. Phys. Org. Chem. 36 (2023) 1–12, https://doi.org/10.1002/poc.4428.
[36] A.V. Marenich, C.J. Cramer, D.G. Truhlar, Perspective on foundations of solvation modeling: the electrostatic contribution to the free energy of solvation, J. Chem. Theory Comput. 4 (2008) 877–887, https://doi.org/10.1021/ct800029c.
[37] S. Maeda, Y. Harabuchi, Y. Ono, T. Taketsugu, K. Morokuma, Intrinsic reaction coordinate: calculation, bifurcation, and automated search, Int. J. Quantum Chem. 115 (2015) 258–269, https://doi.org/10.1002/qua.24757.
[38] Gaussian 16, Revision B.01, M.J. Frisch, G.W. Trucks, H.B. Schlegel, G.E. Scuseria, M.A. Robb, J.R. Cheeseman, G. Scalmani, V. Barone, G.A. Petersson, H. Nakatsuji, X. Li, M. Caricato, A.V. Marenich, J. Bloino, B.G. Janesko, R. Gomperts, B. Mennucci, H.P. Hratchian, J.V. Ortiz, A.F. Izmaylov, J.L. Sonnenberg, D. Williams-Young, F. Ding, F. Lipparini, F. Egidi, J. Goings, B. Peng, A. Petrone, T. Henderson, D. Ranasinghe, V.G. Zakrzewski, J. Gao, N. Rega, G. Zheng, W. Liang, M. Hada, M. Ehara, K. Toyota, R. Fukuda, J. Hasegawa, M. Ishida, T. Nakajima, Y. Honda, O. Kitao, H. Nakai, T. Vreven, K. Throssell, J.A. Montgomery, Jr, J.E. Peralta, F. Ogliaro, M.J. Bearpark, J.J. Heyd, E.N. Brothers, K.N. Kudin, V.N. Staroverov, T.A. Keith, R. Kobayashi, J. Normand, K. Raghavachari, A.P. Rendell, J.C. Burant, S.S. Iyengar, J. Tomasi, M. Cossi, J.M. Millam, M. Klene, C. Adamo, R. Cammi, J.W. Ochterski, R.L. Martin, K. Morokuma, O. Farkas, J.B. Foresman, D.J. Fox, Gaussian, Inc., Wallingford CT, 2016".
[39] G. Bringmann, M. Ochse, M. Michel, Gentrymine B, an N-quaternary ancistrocladus alkaloid: stereoanalysis, synthesis, and biomimetic formation from gentrymine A, Tetrahedron 56 (2000) 581–585, https://doi.org/10.1016/S0040-4020(99)01054-6.
[40] F.P. Gasparro, N.H. Kolodny, N. Barrier, NMR determination of the rotational, J. Chem. Educ. 54 (1977) 258–261 [Online]. Available: papers3://publication/uuid/561DFB3C-4E5D-4A89-BD07-D739AD55C908.
[41] F.H. Allen, O. Kennard, D.G. Watson, L. Brammer, A.G. Orpen, R. Taylor, Tables of bond lengths determined by x-ray and neutron diffraction. Part 1. Bond lengths in organic compounds, J. Chem. Soc. Perkin Trans. 2 (1987) 1–19, https://doi.org/10.1039/P298700000S1.
[42] P.R. Rablen, Computational analysis of the solvent effect on the barrier to rotation about the conjugated C–N bond in methyl *N,N*-dimethylcarbamate, J. Org. Chem. 65 (2000) 7930–7937.
[43] E.A. Basso, R.M. Pontes, Further studies on the rotational barriers of carbamates. An NMR and DFT analysis of the solvent effect for cyclohexyl *N,N*-dimethylcarbamate, J. Mol. Struct. 594 (2002) 199–206 (Theochem).
[44] K.B. Wiberg, P.R. Rablen, D.J. Rush, T.A. Keith, Amides. 3. Experimental and theoretical-studies of the effect of the medium on the rotational barriers for *N,N*-dimethylformamide and *N,N*-dimethylacetamide, J. Am. Chem. Soc. 117 (1995) 4261–4270.